

Kondo state and pressure-induced ferromagnetism in CeZn

H. Kadomatsu, H. Tanaka, M. Kurisu, and H. Fujiwara

Faculty of Science, Hiroshima University, Higashisenda 1-1-89, Hiroshima 730, Japan

(Received 29 October 1985)

A pronounced Kondo anomaly and a transition from antiferromagnetic to ferromagnetic states develop due to a structural phase transition which appears at high pressures above 8 kbar. The magnetic-moment value at 4.2 K and zero field, $0.55\mu_B/\text{Ce}$, in the ferromagnetic state is considerably smaller than that in the antiferromagnetic state at ambient pressure.

I. INTRODUCTION

Dense Kondo anomalies and the valence fluctuations in Ce-based alloys and related compounds have been understood to come from the small energy difference $E_F - E_{4f}$, and the ensuing strong hybridization between the $4f$ level E_{4f} and the Fermi level E_F of the conduction band.¹ Furthermore, crystalline electric field (CEF) effects should be taken into account for a complete understanding, although the analysis becomes very complicated. In order to change or control the magnitude of $E_F - E_{4f}$, especially E_F , pressure will be a very effective and pure external variable, since changing composition or alloying inevitably leads to atomic randomness and heterogeneity.

We have previously studied the magnetic properties of some CsCl-type rare-earth compounds, CeAg,² CeCd,³ CeTi,⁴ and PrAg,⁵ under pressure, where many of them undergo the pressure-induced structural transition from cubic to tetragonal. Since these structural transitions have been considered to come from the ($5d\ 6s$) band Jahn-Teller effect,⁶ pressure brings further splitting of the $5d\ 6s$ bands (degenerate in the cubic phase) resulting in a large change in $E_F - E_{4f}$. This change will certainly influence the Kondo state. In the present work we found in antiferromagnetic CeZn with the cubic CsCl structure that pressure promotes the tetragonal phase with ferromagnetic character and greatly enhances the Kondo anomaly.

II. EXPERIMENTAL

The polycrystalline sample was prepared by sealing the constituent elements in a Ta crucible in Ar atmosphere, melting them at 1200 °C for 3 h and annealing at 500 °C for 1 week in order to homogenize the composition. The clamp-type piston-cylinder pressure cells were used for the measurements of resistivity ρ and magnetization σ at high pressures. Details of the experimental procedures are referred to in our previous articles.^{7,8}

III. RESULTS AND DISCUSSION

In Figs. 1 and 2 are shown the electrical resistivity ρ versus temperature T curves of CeZn at various pressures p 's in temperatures from 2 K up to 60 K (Fig. 1) and up to 300 K (Fig. 2), respectively. In Fig. 1, at ambient pressure $p = 0$ kbar, the change in ρ at the Néel temperature

T_N is rather discontinuous indicating a first-order transition thermodynamically,⁹ where the T_N value ($= 30$ K), indicated by an arrow, was defined as an inflection point in the rapidly falling curve. The T_N value decreases with increasing p . The first-order transition at T_N does not appear at a pressure of 10 kbar. At $p = 12.5$ kbar, two anomalies are seen in the ρ - T curve. (i) A bend at the low-temperature side indicates the appearance of the pressure-induced ferromagnetic state (the Curie temperature T_C), which was confirmed with the magnetic data, as discussed below. The T_C value, indicated by an arrow, was defined as a point of intersection of linear extrapolation of the curves at both sides of the bend. The T_C value initially decreases once and then increases with increasing p . (ii) The broad thermal hysteresis at $p = 12.5$ kbar may be attributed to the structural transition from cubic (high-temperature side) to tetragonal (low-temperature side), judging from the analogous behaviors with other CsCl compounds CeAg,² CeCd,⁵ and LaAg.¹⁰ The transition temperature, denoted by T_M , was defined as the

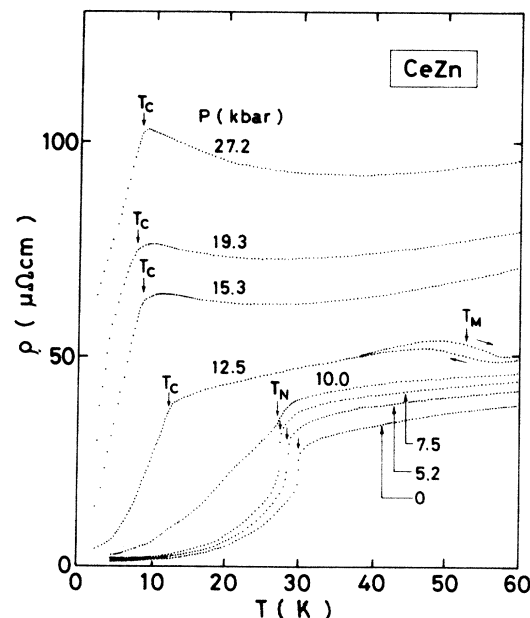


FIG. 1. Electrical resistivity ρ of CeZn versus temperature T (< 60 K) curves at various pressures.

center of gravity of the hysteresis.

The essential result to be mentioned in connection with Fig. 2 is that the Kondo behavior is found to become noticeable at high pressures. It has been reported by Pierre *et al.*⁹ that CeZn displays incipient Kondo behavior at ambient pressure. The definite result at ambient pressure could not be obtained in Fig. 2, but it is found that the slope of the ρ - T curve with temperature in the cubic phase up to 10 kbar above T_N slightly decreases with pressurization indicating the enhancement of Kondo behavior with pressurization. Once the pressure-induced tetragonal phase develops, the overall ρ value markedly increases and the ρ - T curve shows pronounced Kondo behavior with two humps. The result is similar to that obtained for CeCu₂Si₂.¹¹ The dashed curve B in Fig. 2 is the curve at 29 kbar which represents the contribution of 4*f* electrons to ρ . The curve could be obtained in a conventional way by subtracting the phonon part from the observed curve. In the present work the ρ - T curve of nonmagnetic LaZn¹² at ambient pressure (dashed curve A) was temporarily chosen as the phonon part of CeZn. With respect to the thermal hysteresis phenomena at T_M , the hysteresis becomes more evident as pressure increases and dT_M/dp is very large.

Next, the magnetic states at low temperature were examined from the magnetization curve at 4.2 K under pressures as shown in Fig. 3, where the ordinate and abscissa are the magnetization σ in μ_B per Ce and magnetic field H , respectively. At $p=0$ and 4 kbar the magnetization curves are linear from the origin, indicating that the magnetic state is antiferromagnetic up to 4 kbar. At $p=8$ kbar, however, the curve with field hysteresis shows the appearance of spontaneous magnetization; that is, of the pressure-induced ferromagnetic state, although

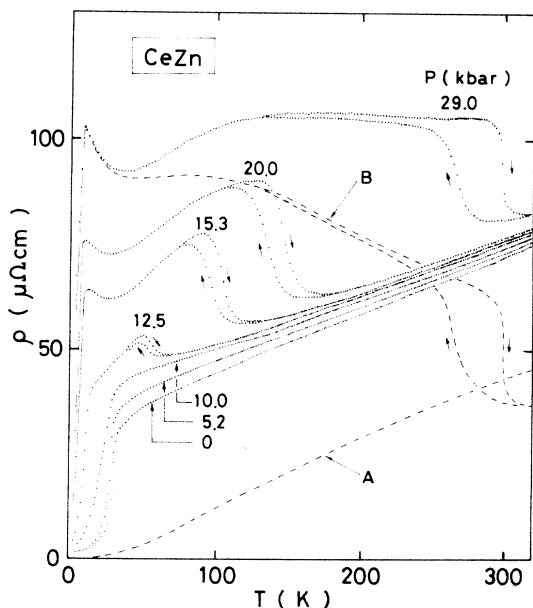


FIG. 2. Electrical resistivity ρ of CeZn versus temperature T (< 300 K) curves at various pressures. The curves A and B are of LaZn at 0 kbar obtained from Ref. 12 and of CeZn at 29 kbar obtained by subtracting curve A, respectively.

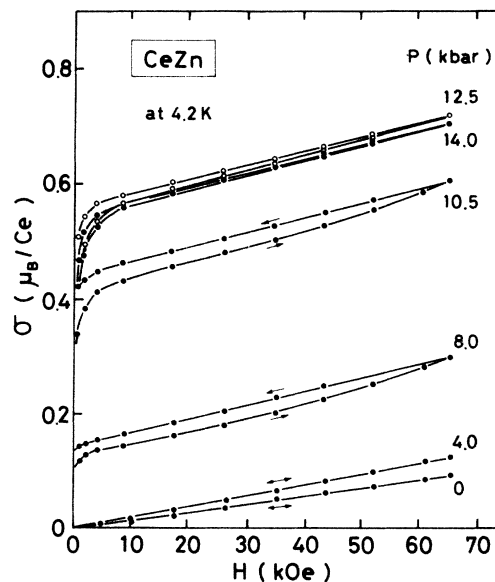


FIG. 3. Magnetization σ at 4.2 K in μ_B/Ce versus magnetic field H curves at various pressures.

the high-field susceptibility is almost the same as that at $p=4$ kbar. With further increase in p , spontaneous magnetization σ_s greatly increases, and the value almost saturates above $p=12.5$ kbar, where σ_s was obtained from the smooth linear extrapolation of the curve back to zero field. The above-mentioned saturated value is about $0.55 \mu_B/\text{Ce}$.

Figure 4 is the pressure-temperature (p - T) magnetic and structural phase diagram of CeZn which has been constructed from our present data. The main points are arranged as follows. (i) The critical pressure p_c , at which the cubic-tetragonal transition appears at 0 K, is 8 kbar and the transition temperature T_M greatly increases with increasing p at a rate of $dT_M/dp = +15$ K/kbar. The values of p_c and dT_M/dp for other CsCl compounds LaAg,¹⁰ CeAg,² and PrAg,⁵ for example, are 4, 2, and 10 kbars for p_c and +17, +18, and +13 K/kbar for

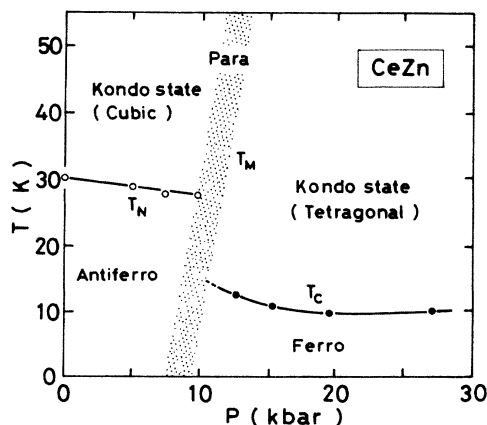


FIG. 4. Pressure-temperature (p - T) magnetic and structural phase diagram. The shaded part denotes the width of the thermal hysteresis of the structural transition (T_M).

dT_M/dp , respectively. (ii) In the low-pressure cubic phase, T_N decreases at a rate of $dT_N/dp = -0.22$ K/kbar. This rate is comparable to -0.17 (CeZn) and -0.2 (CeMg), in the same units, reported by Galera *et al.*,¹³ and to -0.28 (CeTi).⁴ Galera *et al.* have measured T_N up to 6 kbar. (iii) In the pressure-induced tetragonal phase at high pressures, a ferromagnetic state is also induced. With increasing p , the T_C value initially decreases, takes a relatively broad minimum and slightly increases above 20 kbar. (iv) The shaded part denotes the width of thermal hysteresis at T_M or perhaps a mixed region of cubic and tetragonal phases. Therefore, magnetization curves at $p = 8$ and 10.5 kbar in Fig. 3 are those in the mixed region, and curves above 12.5 kbar are in a single tetragonal phase. The disappearance of discontinuity in the ρ - T curve at T_N at 10 kbar in Fig. 1 may be related to the circumstance that the measuring temperature range is just in the mixed region. (v) Once the pressure-induced structural transition develops, the Kondo behavior is pronounced.

Finally discussion will be made on our experimental results: (i) pressure-induced structural transition from cubic to tetragonal and (ii) more conspicuous development of Kondo behavior and a change in the magnetic phase from antiferromagnetic with a large moment value of $1.9 \mu_B/\text{Ce}$ to ferromagnetic with a small moment value of $0.55 \mu_B/\text{Ce}$ after the structural transition.

There is a broad maximum around 80 K in curve B in Fig. 2. This kind of behavior has also been found in the well-known Kondo system CeAl₂,¹⁴ and has been discussed by Cornut and Coqblin¹⁵ as a result of the influence of CEF on the Kondo state. On the basis of their discussion, the CEF Γ_7 - Γ_8 splitting should be roughly equal to 80 K, and this value is comparable with 65 K obtained from neutron diffraction measurements⁹ at ambient pressure in the cubic phase. Further verification of the CEF was checked by the $\ln T$ dependence of ρ . With respect to curve B , the temperature dependences at low ($T_C \sim 30$ K) and high (120~290 K) temperature are linear. The linear dependence is also obtained in the low-temperature range for $p = 15.3$ and 19.3 kbar shown in Fig. 1. The ratio of high-temperature slope of ρ versus $\ln T$ line to the low-temperature slope is about 3.4 in curve B . According to the theoretical estimation,¹⁵ the ratio is 2.3 when the CEF ground state is Γ_8 .

Regarding the variation of the Kondo state with pressure application, Doniach's necklace model¹⁶ has previously been discussed: see Croft *et al.* on CeAl₂ (Ref. 17), DeLong *et al.* on CeIn₃ (Ref. 18), and Eiling and Schilling on CeAg (Ref. 19) in discussing their experimental results. This model is likely to be applied to some parts of our results obtained in the present work, that is, to the antiferromagnetism in the cubic phase, negative dT_N/dp , and enhancement of the Kondo behavior with pressure. Among the properties in the tetragonal phase, however, the appearance of ferromagnetism and nonsensitivity of T_C with further increasing pressure (Fig. 4) are not likely to be explained by the necklace model in its original form. The above-mentioned properties or the coexistence of ferromagnetism and the Kondo state are certainly very interesting and have also been found in CeSi₂.²⁰ But such

behavior is quite infrequent.

The pronounced Kondo behavior in the pressure-induced tetragonal phase in CeZn has been understood as follows in the present work. In CsCl-type rare-earth compounds the Fermi level E_F in the cubic phase has been considered to lie just below a peak of the density of states of the conduction ($5d6s$) band.²¹ When the transition from cubic to tetragonal phases occurs, the degeneracy of the bands will be removed, resulting in a decrease in E_F due to the downward movement of the band bottom. Then the d - f hybridization $|V_{kf}|$ increases and the difference between E_F and E_{4f} , $|E_F - E_{4f}|$, decreases. As a result, the Schrieffer-Wolf-type interaction²²

$$J = - |V_{kf}|^2 / |E_F - E_{4f}|,$$

which is a leading d - f interaction to be considered here, will be enhanced in magnitude. Furthermore, the magnetic f - f interaction between Ce atoms, which suppresses the appearance of the Kondo state, will be reduced, since the magnetic ordering temperature decreases from 30 K to 10 K through the structural distortion. From these circumstances, the pronounced Kondo state in the tetragonal phase at high pressures could be qualitatively understood.

On the bases of the Ruderman-Kittel-Kasuya-Yosida model, the magnetic transition temperature T_N and T_C are expressed by

$$[2\pi N^2 J^2 (g-1)^2 j(j+1) / E_F k_B] \sum_n \exp(-iqR_n) F(2k_F R_n),$$

where $q \neq 0$ for T_N and $q = 0$ for T_C . The decrease in T_N with p cannot be understood as resulting from the pressure dependence of J , which denotes Schrieffer-Wolf-type d - f interaction in the present work. Therefore, the pressure dependence of E_F and $F(2k_F R_n)$, which depend on the band structure, should also be taken into account. The same circumstance will be adopted for the pressure dependence of T_C . The magnetic transition at T_M from antiferromagnetic to ferromagnetic states is mainly attributable to the change in $F(2k_F R_n)$ with p .

Regarding the magnetic moment per Ce atom, the calculated values²³ corresponding to the ground states Γ_8 and Γ_7 are $1.9 \mu_B/\text{Ce}$ and $0.7 \mu_B/\text{Ce}$, respectively. The observed value $1.9 \mu_B/\text{Ce}$ at 4.2 K in the cubic antiferromagnetic phase at ambient pressure indicates that the ground state is Γ_8 in this phase. In contrast, the value in the pressure-induced tetragonal and ferromagnetic phase above p_c was anomalously small, $0.55 \mu_B/\text{Ce}$. We could understand this moment value as follows. The moment value in the cubic antiferromagnetic phase of CeMg (Ref. 23) is large ($\sim 1.85 \mu_B/\text{Ce}$). On the other hand, it is small (0.7 – $0.8 \mu_B/\text{Ce}$) in the tetragonal ferromagnetic phase of CeAg,²⁴ CeCd,²⁵ and CeTi.⁴ So far as these results are concerned, the inversion of the CEF ground state from Γ_8 to Γ_7 caused by the structural transition is likely to be a possible cause of the regularity of the moment value. However, that the circumstance is not simple is derived from our previous results associated with the structural transition in ferromagnetic $(\text{Ce}_{1-x}\text{La}_x)\text{Ag}$ system ($0 \leq x \leq 0.30$).²⁶ There, the moment value in cubic phase for $x > 0.15$ (the transition temperature $T_M < T_C$) does

not change from that in tetragonal phase for $0 \leq x < 0.15$ ($T_M > T_C$). In other words, the inversion of the ground state does not reflect the structural change. Tentative CEF calculations following Wang and Cooper²⁷ have shown that it is possible to have a small σ_s value when the splitting of the Γ_8 ground state due to tetragonal distortion is sufficiently large in comparison with the splitting due to the molecular field. With respect to the Kondo moment compensation, that is the Kondo-type antiparallel coupling between the $4f$ moment and conduction-electron spins, also reduces the moment value. In the present case, however, the remarkably large moment reduction is not easy to explain unless the d - f hybridization is extremely large.

From these circumstances, the moment value may be tied to the magnetic state (ferromagnetic and antiferromagnetic) as well as to the CEF ground state. In order to enlarge on this point qualitatively, the data on the magnetization using single-crystal and neutron diffraction at high pressure, which may give information on the magnetic anisotropy and peculiar spin alignment, will be required.

ACKNOWLEDGMENTS

The present work was supported in part by a Grant-in-Aid for Scientific Research from Ministry of Education, Science and Culture, Japan.

-
- ¹J. M. Lawrence, P. S. Riseborough, and R. D. Parks, Rep. Prog. Phys. **44**, 1 (1981).
²M. Kurisu, H. Kadomatsu, and H. Fujiwara, J. Phys. Soc. Jpn. **52**, 4349 (1983).
³H. Kadomatsu, M. Kurisu, T. Kitai, T. Okamoto, and H. Fujiwara, Phys. Lett. **94A**, 178 (1983).
⁴M. Kurisu, H. Tanaka, H. Kadomatsu, K. Sekizawa, and H. Fujiwara, J. Phys. Soc. Jpn. **54**, 3548 (1985).
⁵H. Kadomatsu, M. Kurisu, and H. Fujiwara, J. Phys. Soc. Jpn. **53**, 1819 (1984).
⁶J. Labbé and J. Friedel, J. Phys. (Paris) **27**, 153 (1966).
⁷H. Fujiwara, H. Kadomatsu, and K. Tohma, Rev. Sci. Instrum. **51**, 1345 (1980).
⁸H. Kadomatsu, K. Tohma, M. Kurisu, and H. Fujiwara, Jpn. J. Appl. Phys. **21**, 140 (1982).
⁹J. Pierre, A. P. Murani, and R. M. Galera, J. Phys. F **11**, 679 (1981).
¹⁰J. S. Schilling, S. Methfessel, and R. N. Shelton, Solid State Commun. **24**, 659 (1977).
¹¹W. Franz, A. Griessel, F. Steglich, and D. Wohlleben, Z. Phys. B **31**, 7 (1978).
¹²H. Peukert and J. S. Schilling, Z. Phys. B **41**, 217 (1981).
¹³R. M. Galera, J. Pierre, J. Voiron, and G. Dampne, Solid State Commun. **46**, 45 (1983).
¹⁴M. N. Francillon, A. Percheron, J. C. Achard, O. Gorochoy, B. Cornut, D. Jérôme, and B. Coqblin, Solid State Commun. **11**, 845 (1972).
¹⁵B. Cornut and B. Coqblin, Phys. Rev. B **5**, 4541 (1972).
¹⁶S. Doniach, in *Valence Instabilities and Related Narrow-Band Phenomena*, edited by R. D. Parks (Plenum, New York, 1977), p. 169.
¹⁷M. C. Croft, R. P. Guertin, L. C. Kupferberg, and R. D. Parks, Phys. Rev. B **20**, 2073 (1979).
¹⁸L. E. DeLong, R. P. Guertin, and S. Foner, Solid State Commun. **32**, 833 (1979).
¹⁹A. Eiling and J. S. Schilling, Phys. Rev. Lett. **46**, 364 (1981).
²⁰H. Yashima, H. Mori, T. Satoh, and K. Kohn, Solid State Commun. **43**, 193 (1982).
²¹A. Hasegawa, B. Bremicker, and J. Kübler, Z. Phys. B **22**, 231 (1975).
²²J. R. Schrieffer and P. A. Wolf, Phys. Rev. **149**, 491 (1966).
²³D. Schmitt, P. Morin, and J. Pierre, J. Magn. Magn. Mater. **8**, 249 (1978).
²⁴M. Kurisu, H. Kadomatsu, and H. Fujiwara, Phys. Lett. **84A**, 496 (1981).
²⁵H. Fujii, T. Kitai, Y. Uwatoka, and T. Okamoto, J. Magn. Magn. Mater. **52**, 428 (1985).
²⁶H. Fujiwara, H. Kadomatsu, and M. Kurisu, J. Magn. Magn. Mater. **31**, 189 (1983).
²⁷Y. L. Wang and B. R. Cooper, Phys. Rev. B **2**, 2607 (1970).